arXiv:gr-qc/0004035v1 12 Apr 2000

Wormholes in Simplicial Minisuperspace

Cristóvão Correia da Silva [1] and *Ruth M. Williams* [2]

DAMTP, Silver Street, Cambridge,
CB3 9EW, England

ABSTRACT

We consider a simplicial minisuperspace modelling wormhole configurations. Such configurations result from a cut and paste procedure on two identical copies of the most relevant triangulation of our universe, namely the cone over α_4, which is the simplest triangulation of S^3. The connecting space where the two copies are glued, acts as the throat of a wormhole connecting two distinct universes. We show that the model contains both Euclidean and Lorentzian classical configurations, although the Euclidean configurations are restricted to very small size, while the Lorentzian ones exist for all sizes. By computing the steepest descents contours associated with the different kind of configurations, and studying the behaviour of the Euclidean action along these contours we are able to conclude that except for a very small range of boundary data, the semiclassical approximation is always valid, which facilitates both the computation and interpretation of the wavefunctions associated to those steepest descents contours. Having computed these semiclassical wavefunctions we could observe that in the case of the microscopic Euclidean wormhole configurations there is a strong prediction of a finite throat, which seems to indicate that such configurations are very likely. For large universe there are only Lorentzian configurations. Some of them have fully complex Euclidean action and the $exp(-ReI)$ acts as the weighting of the Lorentzian

[1] e-mail address : clbc2@damtp.cam.ac.uk
[2] e-mail address : rmw7@damtp.cam.ac.uk

configurations. We find large universes connected by similarly large throats to be strongly favoured.

1 Introduction

In the last decade wormhole configurations have been extensively studied and became more and more "respectable", as they were proved to be almost ubiquitous. There are two main kind of wormholes. In 1988 Coleman , [1], proposed that the existence of microscopic Euclidean wormholes could explain why the cosmological constant is so small in our universe, and eventually yield a probability distribution for all fundamental constants of nature. This launched a flurry of interest on these kind of wormholes,(e.g. [2], [3]), although further results,(e.g. [4], [5]), have cast doubts on the initial claims. On the other hand, macroscopic wormholes connecting large Lorentzian universes have also been a subject of intense study, e.g. [6], [7].

In [6], Hochberg considers a wormhole model that results from taking two copies of (Lorentzian) Friedman-Robertson-Walker universes,

$$ds^2 = -dt^2 + R^2(t)\Big\{\frac{dr^2}{1-kr^2} + r^2(d\theta^2 + \sin\theta^2\, d\phi^2)\Big\} \tag{1}$$

and remove from each of them a $4-$dimensional region of the form $\Omega_{1,2} = \{r_{1,2} \leq a\}$. The resulting $4-$spaces will have identical boundaries $\partial\Omega_{1,2} = \{r_{1,2} = a\}$. By identifying these two boundaries one obtains two FRW spacetimes connected by a wormhole, whose throat is located on their common $\partial\Omega$ boundaries.

There is no need to invoke any arbitrary $3+1$ decomposition of spacetime, usually ADM, as in the case of continuum models. This means that global issues like topology can still be addressed in the simplicial minisuperspace, which is not possible in the continuum versions.

The simplicial framework deals with the universe in a fully $4-$D way, not relying on any specific $3+1$ decomposition of spacetime, usually ADM in the case of continuum models. This means that global issues like topology can still be addressed in the simplicial minisuperspace, which is not possible in the continuum versions. Additionally, it will allow us to use the same simplicial minisuperspace model to study both kinds of wormholes. Simplicial minisuperspace models have proved very reliable in the past by confirming results obtained with the continuum formalism [8], [9], [10]. However, they are at their best when applied to situations which the continuum theory cannot easily handle. Namely, in the study of the effects of generalising the definition of history in quantum gravity, to include conifolds and not just manifolds. See [11],[12], [13]. Furthermore, they can sometimes deliver some unexpected results, like the existence of classical Euclidean solutions for all sizes of the boundary

3−universe, when we consider an arbitrary scalar coupling $\eta R\phi^2$, [14].

2 Simplicial Quantum Gravity

The simplicial framework in QG is usually seen as an approximation to the more fundamental continuum framework. However, it has been argued that at the scales where quantum gravity effects become relevant, it is reasonable to assume that not just energy but even space and time will be discrete. In this way the simplicial framework could even be the more fundamental one.

The basic building block of any simplicial complex is the $n-$simplex.

Definition 2.1 *Given $n+1$ points in R^{n+1}, labelled $v_1, v_2, ..., v_{n+1}$, if these points are affinely independent, then an $n-$dimensional simplex σ^n is the convex hull of these points*

$$\sigma^n = \{x \in R^{n+1} : x = \sum_{i=1}^{n+1} \lambda_i v_i \ where \ \lambda_i \geq 0 \ and \ \sum_{i=1}^{n+1} \lambda_i = 1\} \tag{2}$$

Thus, a $0-$simplex is a vertex, a $1-$simplex is an edge, a $2-$simplex a triangle, etc. Any subset of these vertices also spans a simplex, of lower dimension, which is called a face of σ^n.

From these building blocks we can construct a whole variety of spaces in particular some which by obeying certain natural conditions offer the widest reasonable framework in which to investigate the concept of simplicial geometry. These are called simplicial complexes.

Definition 2.2 *A simplicial complex $(K, \mid K \mid)$ is a topological space $\mid K \mid$ and a collection of simplices K, such that*

- *$\mid K \mid$ is a closed subset of some finite dimensional Euclidean space.*
- *If σ is a face of a simplex in K, then σ is also contained in K.*
- *If σ_a and σ_b are simplices in K, then $\sigma_a \cap \sigma_b$ is a face of both σ_a and σ_b.*
- *The topological space $\mid K \mid$ is the union of all simplices in K.*

By definition the dimension of the simplicial complex is the maximum dimension of any of its simplices.

Each simplex in K is totally described by its vertices. Since a simplicial complex describes both the simplices of the space $\mid K \mid$ and gives the rules for how these building blocks are

connected, then the simplicial complex itself is uniquely determined by the vertices and the rules stating in which simplices they are contained in.

There are several standard topological definitions that extend naturally to simplicial complexes, like

Definition 2.3 *A simplicial complex is compact it it contains a finite number of simplices.*

Definition 2.4 *A simplicial complex is connected if any two of its vertices are connected by a sequence of edges.*

We shall see that in order for it to be possible to define curvature in a complex, (and consequently an action functional for QG), it is essential that this complex be pure, i.e.,

Definition 2.5 *A simplicial $n-$complex, $(K^n, \mid K^n \mid)$, is pure when every lower dimensional simplex in it is contained in at least one $n-$simplex of K^n.*

A natural definition of boundary is also essential. However, it can be shown that the notion of boundary of a complex is meaningful for only a special subset of pure simplicial complexes, which is defined by

Definition 2.6 *A pure simplicial $n-$complex $(K^n, \mid K^n \mid)$, is said to be non-branching if every $(n-1)-$simplex is contained in either one or two $n-$simplices.*

Only now can we define the boundary of a complex as:

Definition 2.7 *The boundary, ∂K^{n-1}, of a pure non-branching simplicial $n-$complex K^n is the complex made up of all $(n-1)-$simplices that are faces of one and only one $n-$simplex of K^n.*

An essential concept for the study of the relationship between continuum spaces and their simplicial representations is that of triangulation

Definition 2.8 *A simplicial complex $(K, \mid K \mid)$ is said to triangulate a smooth space $\mathcal{K}$ if there is an homeomorphism Φ between $\mid K \mid$ and $\mathcal{K}$.*

Conventionally, if $\mathcal{K}$ is an $n-$sphere then it is said that $(K, \mid K \mid)$ is a simplicial $n-$sphere, the same for an $n-$ball, etc. In the topological sense we can say that K is the simplicial counterpart of $\mathcal{K}$.

What characterises a continuum topological manifold is the fact that all its points have neighbourhoods homeomorphic to open sets in R^n, like an open ball B^n. So the definition of the simplicial version of a continuum manifold is dependent on the definition of the simplicial equivalent of boundary of a point. Only then can the local topology of the complexes be studied.

Definition 2.9 *Given a simplicial complex $(K^n, \mid K^n \mid)$, the combinatorial star of a vertex $v \in K^n$, denoted $St(v)$, is the complex consisting of all the $n-$simplices of K^n that contain v.*

Definition 2.10 *Given a simplicial complex $(K^n, \mid K^n \mid)$, the combinatorial link of a vertex $v \in K^n$, denoted $L(v)$, is the complex consisting of all the simplices that are in $St(v)$ but do not contain v itself.*

The star of a vertex is very much like the neighbourhood of a point in a continuum framework. So we expect that the defining characteristic of the simplicial analogues of manifolds to be that the star of each vertex be homeomorphic to an open ball B^n, which is equivalent to say that its star is a simplicial open $n-$ball. However it is customary to reformulate these conditions in terms of links and not stars.

It is easy to see that to say that $St(v)$ is a simplicial open $n-$ball is equivalent to say that $L(v)$ is a simplicial $(n-1)$-sphere. And so we will restate the "manifold condition" as that the combinatorial link of every vertex be homeomorphic to an $(n-1)$-sphere, i.e., $L(v)$ be a simplicial $(n-1)-$sphere.

For technical reasons the previous conditions are still not enough for the resulting simplicial complexes to have the same properties as continuum manifolds. One last condition is needed.

Definition 2.11 *A simplicial $n-$complex $(K^n, \mid K^n \mid)$ is said to be strongly connected if any two simplices of K^n can be connected by a sequence of $n-$simplices each intersecting along some $(n-1)$-simplex.*

We can now define the simplicial counterparts of smooth manifolds:

Definition 2.12 *A combinatorial $n-$manifold $\mathcal{M}^n$, is an $n-$dimensional simplicial complex such that*

- *It is pure.*
- *It is non-branching.*
- *Any two $n-$simplices can be connected by a sequence of $n-$simplices, each intersecting along some $(n-1)-$simplex.*
- *The link of every vertex is a simplicial $(n-1)-$sphere.*

Note that there are simplicial complexes that are homeomorphic to topological manifolds but are not combinatorial manifolds. The definition of combinatorial manifold carries more structure than simply the topology.

2.1 Simplicial Geometry

We have so far been concerned solely with the topological and combinatorial aspects of simplicial quantum gravity. We shall now focus on the geometric issues.

The simplest way to describe a geometry on an any pure non-branching simplicial complex K^n is to use the Regge formalism:

- 1)We require the metric on the interior of each $n-$simplex of K^n to be flat.
- 2) We then assign edge lengths to each edge of K^n. Not every assignment of edge lengths is consistent with the simplices having flat interiors. The triangle inequalities and their higher dimensional analogues must be satisfied. Necessary and sufficient conditions for this to happen are that the squared volumes of all $k-$simplices, with $k = 2, 3, ...n$, must be positive.

The metric information, which in the continuum spaces is contained on the metric tensor $g_{\mu\nu}$, is imprinted on a simplicial complex, K^n, via an assignment of its squared edge lengths.

$$g_{\mu\mu}(x) \rightarrow g_{ij}(\{s_k\}) = \frac{s_{0i} + s_{0j} - s_{ij}}{2} \tag{3}$$

where 0 is just an arbitrary vertex of K^n, and s_{ij} is the square edge length of the edge $[ij]$.

Note that in the simplicial framework the metric degrees of freedom are now the squared edge lengths s_k. This means that all geometric quantities should be expressible in terms of them.

Since by definition the metric inside each $n-$simplex is flat the curvature in a simplicial complex cannot reside there. Instead it is located at the $(n-2)-$simplices of the complex. The curvature associated with each $(n-2)-$simplex is measured by what is called its deficit angle, whose expression is slightly different according to whether the $(n-2)-$simplex is located in the interior or on the boundary of the complex:

For an interior $(n-2)-$simplex, σ_i^{n-2}, the deficit angle is

$$\theta(\sigma_i^{n-2}) = 2\pi - \sum_{\sigma^n \in St(\sigma_i^{n-2})} \theta_d(\sigma_i^{n-2}, \sigma^n) \tag{4}$$

where $\theta_d(\sigma_i^{n-2}, \sigma_n)$ is called the dihedral angle of σ_i^{n-2} associated with σ_i^n, and is the angle between the the two $(n-1)$-simplices that belong to σ_i^n and intersect at σ_i^{n-2}).

For a $(n-2)-$simplex, σ_b^{n-2}, on the boundary of the complex, the deficit angle is

$$\psi(\sigma_b^{n-2}) = \pi - \sum_{\sigma^n \in St(\sigma_b^{n-2})} \theta_d(\sigma_b^{n-2}, \sigma^n) \tag{5}$$

It is easy to see why the previous definitions of curvature are only valid for pure complexes. Only in a pure complex can we be sure that any $(n-2)-$simplex is indeed contained in some $n-$simplex.

Following Regge, the continuum Einstein action can be discretized for any pure non-branching complex as

$$\begin{aligned} I[K^n, \{s_k\}] &= \frac{-2}{16\pi G} \sum_{\sigma_i^{n-2}} V_{n-2}(\sigma_i^{n-2})\theta(\sigma_i^{n-2}) + \frac{2\Lambda}{16\pi G} \sum_{\sigma^n} V_n(\sigma^n) \\ &- \frac{2}{16\pi G} \sum_{\sigma_b^{n-2}} V_{n-2}(\sigma_b^{n-2})\psi(\sigma_b^{n-2}) \end{aligned} \tag{6}$$

where $V_p(\sigma^p)$ is the $p-$ volume of the $p-$simplex, σ_p.

It is easy to see that all the volumes as all the deficit angles can be written as functions of the squared edge lengths $\{s_k\}$. See [9] for their explicit form.

We can now write the wavefunction of the universe in simplicial quantum cosmology as

$$\Psi[\partial K^{n-1}, \{s_b\}] = \sum_{K^n} \int_C D\{s_i\} e^{-I[K^n, \{s_i\}, \{s_b\}]} \tag{7}$$

where

- $\{s_i\}$ are the squared lengths of the interior edges
- $\{s_b\}$ are the squared lengths of the boundary edges
- The kind sum over complexes K^n depends on the boundary conditions one adheres to. For example the equivalent of Hartle-Hawking's no boundary proposal would be to consider a sum over all compact combinatorial $n-$manifolds $\mathcal{M}^n$ whose only boundary is $\partial\mathcal{M}^{n-1}$, and over all simplicial $n-$geometries $\{s_k\}$ that have boundary edges with squared lengths $\{s_b\}$

Note that the while in the continuum we had a functional metric integral, we now have a well defined product of integrals over edge lengths. So it seems we have removed the problems related to issues of gauge fixing and renormalisation associated with defining the measure of the space of metrics. However, such problems reappear in any attempt to take the continuum limit of this Regge integral. Similarly the functional integral associated with the the scalar field now becomes a product of well defined simple integrals over the value of the field in each interior vertex.

3 Simplicial Minisuperspace

A simplicial minisuperspace approximation (in a pure gravity model) consists of imposing two kinds of restrictions on the quantities being summed over in (7). Namely, it involves singling out a particular complex or family of complexes and singling out a few edge lengths, by making all others a function of them. We are thus imposing restrictions of a topological and geometrical nature.

In our case we will have:

$$\sum_{K^n} \longrightarrow W^4$$

$$\{s_i\} \longrightarrow s_i$$

$$\{s_b\} \longrightarrow a, b$$

Where W^4 and the other restrictions will be explained in more detail in the next section.

3.1 Topology Restrictions

Consider two identical copies of the combinatorial manifold $\mathcal{C} = 0 * \alpha_4$ we used in [14] as a model of our universe. We shall denote them $\mathcal{C}_1$, and $\mathcal{C}_2$. As we have shown in the previous chapter these models provide a good approximation to the wavefunction of the universe, by predicting classical Lorentzian spacetime in the late universe. So we can consider them two separate but identical 4−D universes.

We now proceed to construct a connection between them acting as a wormhole connecting these two universes. To do so note that $\mathcal{C}_1$ is composed of five 4−simplices:

$$\mathcal{C}_1 = [01234], [01345], [01235], [01245], [02345]$$

Remember that the 4−simplex [12345] does not belong $\mathcal{C}_1$ because the triangulation α_4 of the 3−sphere, is just the surface of [12345].

Similarly $\mathcal{C}_2$ is composed of five equivalent 4−simplices,

$$\mathcal{C}_2 = [0'1'2'3'4'], [0'1'3'4'5'], [0'1'2'3'5'], [0'1'2'4'5'], [0'2'3'4'5']$$

These two copies of our model universe are displayed in figure 5.1.

If we now remove one of these identical 4−simplices from each complex, say, [02345] and $[0'2'3'4'5']$, and then glue the resulting complexes through the identification of the vertices $0 = 0'$, $2 = 2'$, $3 = 3'$, $4 = 4'$ and $5 = 5'$, then we have connected the two independent 4−D universes, through a 3−D throat, thus modelling a wormhole. The resulting 4−complex shall be denoted as W^4, and the identified vertices will be denoted as $0, 2, 3, 4, 5$, see figure 5.2. There are of course two non-identified vertices 1 and $1'$. Note also that given the identification $0 = 0'$, the complex W^4 has only one interior vertex. W^4 is composed of eight 4−simplices:

$$W^4 = [01234], [01235], [01345], [01245], [01'234], [01'235], [01'245], [01'345]$$

Note that the 4−simplex [02345] does not exist in W^4. Furthermore, W^4 has only one boundary, the 3−complex made up of the following 3−simplices:

$$\begin{aligned} \partial W^4 &= [1234], [1'234], [1235], [1'235], [1245], [1'245], \\ &\quad [1345], [1'345]. \end{aligned} \tag{8}$$

The 3−simplex [2345] does not exist in W^4, since it belongs only to [12345], [1′2345] and [02345] and by definition W^4 does not contain these 4−simplices, and since we want W^4 to be pure and non branching all 3−simplices in W^4 have to belong either to one or two 4−simplices. However, the four triangles that form the surface of [2345], i.e., [234], [235], [245] and [345], do belong to W^4.

We can thus conclude that the boundary ∂W^4 is a combinatorial 3−manifold. Indeed if we compute the links of its vertices all are homeomorphic to S^2.

$$L_{\partial W}(1) = L(1') = [234] \cup [235] \cup [245] \cup [345] \tag{9}$$

So we see that the links of the vertices 1 and 1′ are simply the surface of a tetrahedron [2345].

$$L_{\partial W}(2) = [134] \cup [1'34] \cup [135] \cup [1'35] \cup [145] \cup [1'45] \tag{10}$$

Thus, the link of vertex 2 is just the surface of an hexahedron. The same is true for vertices 3, 4 and 5. This is only valid because [2345] does not belong to W^4. If that was not the case the link of vertex 2 would not be homeomorphic to S^2 and the boundary ∂W^4 would not be a 3−manifold.

The throat T^3 of the wormhole is the 3−D surface of the 4−simplex [02345] without [2345] . See figure 3. It is a combinatorial 3−manifold constituted by the 3−simplices:

$$T^3 = [0234], [0345], [0235], [0245]$$

3.2 Geometry

For simplicity and since there is still only one interior vertex, we shall assume that all interior edge lengths are equal, and their squared values are s_i.

$$s_{01} = s_{01'} = s_{02} = s_{03} = s_{04} = s_{05} = s_i$$

However, it is essential that not all boundary edge lengths are the same if we want to separate the evolution of the whole boundary 3−universe from that of the wormhole's throat. So we shall assume that all boundary edges belonging to the throat T^3 will have squared lengths b,

$$s_{23} = s_{24} = s_{25} = s_{34} = s_{35} = s_{45} = b$$

while all the other boundary edges have square edge length a.

4 Minisuperspace Wavefunction

Having defined our simplicial minisuperspace model our objective is now to evaluate the wavefunction associated with it. Although the 4−complex is now somewhat more complicated we simplify the model by not considering any matter sector. The general formulae obviously still apply. So the minisuperspace wavefunction will be given by

$$\Psi[a,b] = \int_C Ds_i e^{-I[s_i,a,b]} \tag{11}$$

To implement this expression we start by computing the Euclideanized Regge action for the model. Since we have no matter sector we have simply

$$\begin{aligned} I[W^4,a,b] &= \frac{-2}{16\pi G}\sum_{\sigma_2^i} V_2(\sigma_2^i)\theta(\sigma_2^i) + \frac{2\Lambda}{16\pi G}\sum_{\sigma_4} V_4(\sigma_4) \\ &- \frac{2}{16\pi G}\sum_{\sigma_2^b} V_2(\sigma_2^b)\psi(\sigma_2^b) \end{aligned} \tag{12}$$

where:

- σ_k denotes a $k-$simplex belonging to the set Σ_k of all $k-$simplices in W^4.
- $\theta(\sigma_2^i)$, is the deficit angle associated with the interior 2−simplex $\sigma_2^i = [ijk]$
- $\psi(\sigma_2^b)$ is the deficit angle associated with the boundary 2−simplex σ_2^b
- $V_k(\sigma_k)$ for $k = 2,3,4$ is the $k-$volume associated with the $k-$simplex, σ_k.

As before all these quantities can be expressed in terms of the squared edge lengths, s_i, a and b, according to the expressions in appendix 1.

- With our choice of edge lengths, all eight 4−simplices that compose W^4 are of the same type, and their 4−volume can be computed as

$$V_4(\sigma_4) = \frac{b^2}{48}\sqrt{3\frac{as_i}{b^2} - \frac{s_i}{b} - \frac{3}{4}\frac{a^2}{b^2}} \tag{13}$$

- There is only one type of boundary 3−simplex. The eight of them, can be denoted as $[aaabbb]$, i.e., they have three edges of squared length a and three edges of squared length b. They all have the same volume. As an example take [1234], its volume is

$$V_3(\sigma_3^b) = \frac{\sqrt{3}\, b^{3/2}}{12}\sqrt{\frac{a}{b} - \frac{1}{3}} \tag{14}$$

- As for interior 3−simplices there are two types. Type I can be described as $[aabs_is_is_i]$, of which [0123] is an example. There are twelve of them and they all have the same volume

$$V_3(\sigma_3^{Ii}) = \frac{b^{3/2}}{12}\sqrt{4\frac{as_i}{b^2} - \frac{s_i}{b} - \frac{a^2}{b^2}} \tag{15}$$

  There are four more interior 3−simplices, of type II, which are [0234], [0235], [0345], and [0245]. They all have the same volume

$$V_3(\sigma_3^{IIi}) = \frac{\sqrt{3}\; b^{3/2}}{12}\sqrt{\frac{s_i}{b} - \frac{1}{3}} \tag{16}$$

- We have twelve boundary triangles of the kind $[aab]$, which we shall call type I, e.g., [123] and they all have the same area

$$V_2(\sigma_2^{Ib}) = \frac{b}{2}\sqrt{\frac{a}{b} - \frac{1}{4}} \tag{17}$$

  and four boundary triangles of the kind $[bbb]$, type II, e.g., [234] whose area is

$$V_2(\sigma_2^{IIb}) = \frac{\sqrt{3}}{4}b \tag{18}$$

- There are also two kinds of interior triangles. Type I includes the ones of the kind $[as_is_i]$, e.g., [012]. They all the same area

$$V_2(\sigma_2^{Ii}) = \frac{a}{2}\sqrt{\frac{s_i}{a} - \frac{1}{4}} \tag{19}$$

  There are six more of type II, $[bs_is_i]$, like [023], whose area is

$$V_2(\sigma_2^{IIi}) = \frac{b}{2}\sqrt{\frac{s_i}{b} - \frac{1}{4}} \tag{20}$$

For simplicity from now on we shall be working with rescaled metric variables:

$$\eta = \frac{s_i}{b} \tag{21}$$

$$\alpha = \frac{a}{b} \tag{22}$$

$$T = \frac{H^2 b}{l^2} \tag{23}$$

where $H^2 = l^2\Lambda/3$, and $l^2 = 16\pi G$ is the Planck length. We shall work in units where $c = \hbar = 1$.

Since we have two types of interior and boundary triangles we can expect at least four different deficit angles. The deficit angle associated with all eight interior triangles of type I is the same:

$$\theta(\sigma_2^{Ii}) = 2\pi - 3\arccos\left\{\frac{1}{2}\frac{(4\alpha-2)\eta-\alpha^2}{(4\alpha-1)\eta-\alpha^2}\right\} \tag{24}$$

Similarly, all six interior triangles of type II have the same deficit angle

$$\theta(\sigma_2^{IIi}) = 2\pi - 4\arccos\left\{\frac{2\eta-\alpha}{2\sqrt{3\eta-1}\sqrt{(4\alpha-1)\eta-\alpha^2}}\right\} \tag{25}$$

As for the deficit angles associated with the boundary triangles, we can show that all twelve boundary triangles of type I have the same deficit angle

$$\psi(\sigma_2^{Ib}) = \pi - 2\arccos\left\{\frac{\alpha}{2\sqrt{3\alpha-1}\sqrt{(4\alpha-1)\eta-\alpha^2}}\right\} \tag{26}$$

the remaining four boundary triangles of type II also have the same deficit angle

$$\psi(\sigma_2^{IIb}) = \pi - 2\arccos\left\{\frac{(3\alpha-2)}{2\sqrt{3\alpha-1}\sqrt{3\eta-1}}\right\} \tag{27}$$

We can now write the explicit expression of the Regge action for this model:

$$\begin{aligned} I[\eta,T,\alpha] &= -\frac{T}{H^2}\Big\{8\sqrt{\alpha}\sqrt{\eta-\frac{\alpha}{4}}\Big[2\pi - 3\arccos\Big(\frac{1}{2}\frac{(4\alpha-2)\eta-\alpha^2}{(4\alpha-1)\eta-\alpha^2}\Big)\Big] \\ &+ 6\sqrt{\eta-1/4}\Big[2\pi - 4\arccos\Big(\frac{2\eta-\alpha}{2\sqrt{3\eta-1}\sqrt{(4\alpha-1)\eta-\alpha^2}}\Big)\Big] \\ &+ 6\sqrt{4\alpha-1}\Big[\pi - 2\arccos\Big(\frac{\alpha}{2\sqrt{3\alpha-1}\sqrt{(4\alpha-1)\eta-\alpha^2}}\Big)\Big] \end{aligned}$$

$$
\begin{aligned}
&+ \quad 2\sqrt{3}\Big[\pi - 2\arccos\Big(\frac{(3\alpha-2)}{2\sqrt{3\alpha-1}\sqrt{3\eta-1}}\Big)\Big] \\
&+ \quad \frac{T^2}{H^2}\Big\{\alpha\sqrt{\frac{(3\alpha-1)\eta}{\alpha^2}-\frac{3}{4}}\Big\}
\end{aligned}
\tag{28}
$$

4.1 Analytic Study of The Action

For obvious physical reasons we require the boundary edge lengths a and b, and thus T and α, to be real and positive. On the other hand since we are only interested in geometries in which the boundary three-metric is positive definite, we must require that the volume of the boundary three-simplices be positive which is equivalent to requiring that $\alpha > \frac{1}{3}$.

However, as pointed out in [15], for it to be possible for the wavefunction of the universe to predict a classical Lorentzian Universe the integration contour considered must be over complex metrics. Thus we are lead to consider η as being a complex variable, and the analytic study of the action as a function of a complex variable η is essential.

The first thing to do is to identify the branch points of the action. Terms like $\sqrt{z-z_0}$, are double-valued and have a square-root branch point at $z = z_0$. In order to make this term continuous we need to cut the complex plane. The most common branch cut is simply $(-\infty, z_0]$.

So we see that the Euclidean action has 3 square-root branch points located at:

$$
\eta_0 = \frac{3}{4}\frac{\alpha^2}{3\alpha-1}
$$

$$
\eta_2 = \frac{\alpha}{4}
$$

$$
\eta_3 = \frac{1}{4}
$$

On the other hand a term like $\arccos u(z)$, is infinitely many-valued and has branch points at $u(z) = +1, -1$, and at $u(z) = \infty$. The associated branch cuts are usually taken to be $(-\infty, -1] \cup [1, +\infty)$.

Since

$$
\arccos u(z) = -i\log\Big(u(z) + \sqrt{u(z)^2 - 1}\Big)
$$

then we see that there are logarithmic singularities when $u(z) = \infty$. The table below shows the logarithmic branching points and infinities associated with the dihedral angles, where

$$\eta_1 = \frac{\alpha^2}{4\alpha - 1}$$

Dihedral angles	$+1$	-1	∞
$\theta(\sigma_2^{Ii})$	$1/4$, η_0	$1/4$, η_0	$1/3$
$\theta(\sigma_2^{IIi})$	$\alpha/4$	η_0	η_1
$\theta(\sigma_2^{Ib})$	η_0	η_0	η_1
$\theta(\sigma_2^{IIb})$	η_0	η_0	$1/3$

In order to determine which branch cuts to take we need to know the relative values of these critical points, but those are dependent on the value of the boundary parameter α. There are however some relations that are always valid for all $\alpha > 1/3$

$$\eta_0 > \frac{\alpha}{4}, \frac{1}{3}$$
$$\eta_1 > \frac{1}{4}$$
$$\eta_0 > \eta_1$$
$$\eta_1 > \frac{\alpha}{4}$$

So we see that the only indeterminates are $min(\eta_1, \frac{1}{3})$, $min(\frac{\alpha}{4}, \frac{1}{4})$ and $min(\frac{\alpha}{4}, \frac{1}{3})$.

However, it is easy to see that the first two are just the same $min(\alpha, 1)$, and the third can of course be rewritten as $min(\alpha, \frac{4}{3})$.

Thus, we have three different regions

- $\frac{1}{3} < \alpha < 1$, where $\frac{\alpha}{4} < \frac{1}{4} < \eta_1 < \frac{1}{3} < \eta_0$
- $1 < \alpha < \frac{4}{3}$, where $\frac{1}{4} < \frac{\alpha}{4} < \frac{1}{3} < \eta_1 < \eta_0$
- $\frac{4}{3} < \alpha < +\infty$, where $\frac{1}{4} < \frac{1}{3} < \frac{\alpha}{4} < \eta_1 < \eta_0$

So when we consider all the cuts associated to all the terms we shall take as total branch cut $(-\infty, \eta_0]$. This also takes care of the logarithmic singularity at $\eta = 1/3$.

This cut leads to a continuous action function, in the complex plane with a cut $(-\infty, \eta_0]$. However this function is still infinitely many-valued. As in the previous chapters in order to

remove this multivaluedness we redefine the domain where the action is defined, from the complex plane to the Riemann surface associated with I. The infinite multivaluedness of the action reflects itself in I having an infinite number of branches with taking different values. The Riemann surface, $\mathbf{R}$ is composed by an infinite number of identical sheets, $\mathbb{C}-(-\infty,\frac{3}{8}]$, one sheet for each branch of I.

The first sheet $\mathbb{C}_1$ of the action is defined as the sheet where the terms in $\arccos(z)$ assume their principal values. That is the sheet where the action takes the form (29), and so $I^I[\eta,\alpha,T]=I[\eta,\alpha,T]$. When we continue the action in ξ around one or more branch points, we will leave this first sheet and emerge in some other sheet of the Riemann surface. Only a few of these other sheets are relevant to us.

When we encircle all five branch points we leave the first sheet and enter what we shall call the second sheet. It is easy to see that if we cross the branch cut $(-\infty,\eta_0]$, somewhere between $-\infty$ and the smallest branch point ($\alpha/4$ or $1/4$, according to the value of α) all terms of the action change their sign in this new sheet. Thus, the action in the second sheet differs by an overall minus sign relative to the action in the first sheet, $I^{II}[\eta,\alpha,T]=-I^I[\eta,\alpha,T]$.

However, we shall see that the steepest descents (SD) contours yielding the desired wave-functions of the universe cross the branch cuts at other locations, thus emerging onto other sheets. For example, when $\alpha>4/3$, if we take a contour that encircles the branch point $1/4$, then at the first crossing of the branch cut, somewhere in $(-\infty,1/4]$, we go from the first sheet $\mathbb{C}_1$ to the second $\mathbb{C}_2$, and the action changes overall sign. Continuing in such a way that we again cross the branch cut, now between $1/4$ and the nearest branch point $1/3$, the contour enters what we shall call the third sheet. By carefully studying the behaviour of each term at the branch crossing, taking into account the branch cuts associated to each of them, we conclude that in this third sheet, $\mathbb{C}_3$, the action is

$$\begin{aligned}
I^{III}[\eta,T,\alpha] &= -\frac{T}{H^2}\Bigg\{8\sqrt{\alpha}\sqrt{\eta-\frac{\alpha}{4}}\Bigg[2\pi-3\arccos\left(\frac{1}{2}\frac{(4\alpha-2)\eta-\alpha^2}{(4\alpha-1)\eta-\alpha^2}\right)\Bigg] \\
&+ -6\sqrt{\eta-1/4}\Bigg[2\pi+4\arccos\left(\frac{2\eta-\alpha}{2\sqrt{3\eta-1}\sqrt{(4\alpha-1)\eta-\alpha^2}}\right)\Bigg] \\
&+ 6\sqrt{4\alpha-1}\Bigg[\pi-2\arccos\left(\frac{\alpha}{2\sqrt{3\alpha-1}\sqrt{(4\alpha-1)\eta-\alpha^2}}\right)\Bigg] \\
&+ 2\sqrt{3}\Bigg[\pi-2\arccos\left(\frac{(3\alpha-2)}{2\sqrt{3\alpha-1}\sqrt{3\eta-1}}\right)\Bigg] \qquad (29)
\end{aligned}$$

$$
+ \quad \frac{T^2}{H^2}\Big\{\alpha\sqrt{\frac{(3\alpha-1)\eta}{\alpha^2}-\frac{3}{4}}\,\Big\}
$$

There is another important case, (still when $\alpha > 4/3$), in which the SD contour encircles another branch point, namely $\alpha/4$. In this case we are confronted with a contour that starting on the first sheet, crosses the branch cut between $1/3$ and $\alpha/4$, encircles $\alpha/4$ and crosses the cut, once again somewhere between $\alpha/4$ and η_1. During the first crossing if we pay attention to the branch cuts in each term of the action, all terms of the action change their signs except the one associated with $\arccos\theta(\sigma_b^{II})$, and so we end up at what we shall call the fourth sheet $\mathbf{C}_4$, where the action is

$$
\begin{aligned}
I^{IV}[\eta,T,\alpha] \;=\; & \frac{T}{H^2}\Big\{8\sqrt{\alpha}\sqrt{\eta-\frac{\alpha}{4}}\Big[2\pi-3\arccos\Big(\frac{1}{2}\frac{(4\alpha-2)\eta-\alpha^2}{(4\alpha-1)\eta-\alpha^2}\Big)\Big] \\
+ \; & 6\sqrt{\eta-1/4}\Big[2\pi-4\arccos\Big(\frac{2\eta-\alpha}{2\sqrt{3\eta-1}\sqrt{(4\alpha-1)\eta-\alpha^2}}\Big)\Big] \\
+ \; & 6\sqrt{4\alpha-1}\Big[\pi-2\arccos\Big(\frac{\alpha}{2\sqrt{3\alpha-1}\sqrt{(4\alpha-1)\eta-\alpha^2}}\Big)\Big] \\
+ \; & 2\sqrt{3}\Big[-\pi-2\arccos\Big(\frac{(3\alpha-2)}{2\sqrt{3\alpha-1}\sqrt{3\eta-1}}\Big)\Big] \\
- \; & \frac{T^2}{H^2}\Big\{\alpha\sqrt{\frac{(3\alpha-1)\eta}{\alpha^2}-\frac{3}{4}}\,\Big\}
\end{aligned}
\tag{30}
$$

We then proceed to the second branch crossing somewhere between $\alpha/4$ and η_1, from where we emerge onto yet another sheet, $\mathbf{C}_5$. Once more if we pay attention to the branch cuts in each term of the action we can conclude that the action in this fifth sheet takes the form

$$
\begin{aligned}
I^{V}[\eta,T,\alpha] \;=\; & -\frac{T}{H^2}\Big\{-8\sqrt{\alpha}\sqrt{\eta-\frac{\alpha}{4}}\Big[2\pi+3\arccos\Big(\frac{1}{2}\frac{(4\alpha-2)\eta-\alpha^2}{(4\alpha-1)\eta-\alpha^2}\Big)\Big] \\
+ \; & 6\sqrt{\eta-1/4}\Big[2\pi-4\arccos\Big(\frac{2\eta-\alpha}{2\sqrt{3\eta-1}\sqrt{(4\alpha-1)\eta-\alpha^2}}\Big)\Big] \\
+ \; & 6\sqrt{4\alpha-1}\Big[\pi-2\arccos\Big(\frac{\alpha}{2\sqrt{3\alpha-1}\sqrt{(4\alpha-1)\eta-\alpha^2}}\Big)\Big] \\
+ \; & 2\sqrt{3}\Big[\pi-2\arccos\Big(\frac{(3\alpha-2)}{2\sqrt{3\alpha-1}\sqrt{3\eta-1}}\Big)\Big] \\
+ \; & \frac{T^2}{H^2}\Big\{\alpha\sqrt{\frac{(3\alpha-1)\eta}{\alpha^2}-\frac{3}{4}}\,\Big\}
\end{aligned}
\tag{31}
$$

We have just examined two cases that will be relevant when dealing with the SD contours, however, the lesson to be taken is that given the high number of branch points, the Riemann surface of the action is highly non-trivial and we must consider the changing form of the action along its sheets.

4.2 Asymptotic Behaviour of the Action

Once more the asymptotic behaviour of the action with respect to the integration variable, η, is essential to the study of the convergence of the path integral yielding the wavefunction. Only after we know this asymptotic behaviour can we guarantee that the steepest descents contour is indeed dominated by the correct classical solutions. However from what we have seen in the previous chapter we must study this asymptotic behaviour not just in the first sheet but in all others where the SD contours are liable to go to infinity.

It is easy to see that in the first sheet, the asymptotic behaviour of the action is

$$I^I[\eta \to \infty, \alpha, T] \sim \frac{\sqrt{3\alpha - 1}}{H^2} T \Big[T - T^I_{crit}(\alpha) \Big] \sqrt{\eta} \tag{32}$$

where

$$\begin{aligned} T^I_{crit}(\alpha) &= \frac{8\sqrt{\alpha}}{\sqrt{3\alpha - 1}} \Big[2\pi - 3 \arccos\Big(\frac{2\alpha - 1}{4\alpha - 1} \Big) \Big] \\ &+ \frac{6}{\sqrt{3\alpha - 1}} \Big[2\pi - 4 \arccos\Big(\frac{1}{\sqrt{3}\sqrt{4\alpha - 1}} \Big) \Big]; \end{aligned} \tag{33}$$

for the third sheet we have

$$I^{III}[\eta \to \infty, \alpha, T] \sim \frac{\sqrt{3\alpha - 1}}{H^2} T (T - T^{III}_{crit}) \sqrt{\eta} \tag{34}$$

where now

$$\begin{aligned} T^{III}_{crit}(\alpha) &= \frac{8\sqrt{\alpha}}{\sqrt{3\alpha - 1}} \Big[2\pi - 3 \arccos\Big(\frac{2\alpha - 1}{4\alpha - 1} \Big) \Big] \\ &- \frac{6}{\sqrt{3\alpha - 1}} \Big[2\pi + 4 \arccos\Big(\frac{1}{\sqrt{3}\sqrt{4\alpha - 1}} \Big) \Big] \end{aligned} \tag{35}$$

and finally for the fifth sheet

$$I^V[\eta \to \infty, \alpha, T] \sim \frac{\sqrt{3\alpha - 1}}{H^2} T (T - T^V_{crit}) \sqrt{\eta} \tag{36}$$

where now

$$T^V_{crit}(\alpha) = -\frac{8\sqrt{\alpha}}{\sqrt{3\alpha-1}}\left[2\pi + 3\arccos\left(\frac{2\alpha-1}{4\alpha-1}\right)\right] + \frac{6}{\sqrt{3\alpha-1}}\left[2\pi - 4\arccos\left(\frac{1}{\sqrt{3}\sqrt{4\alpha-1}}\right)\right]. \tag{37}$$

In figure 4 we see the plot of $T^I_{crit}(\alpha)$. It becomes infinite as α approaches 1/3, which corresponds to the vanishing of the volume of σ_3^{Ib}. However, for all other values of α away from 1/3 it quickly settles down at its asymptotic value $Tcrit^I(+\infty) = 14.51$.

In the case of T^{III}_{crit} it becomes $-\infty$ when $\alpha \to 1/3$, and as α increases it becomes positive, having the same asymptotic value as T^I_{crit}, which is its upper bound. As for T^V_{crit} it is always negative, whatever the value of α.

5 Classical Solutions

Since the complex W^4 is composed by eight equivalent 4−simplices, the metric of the complex will coincide with the metric of each simplex. The simplicial metric is then

$$g_{ij}(\{s_k\}) = \frac{s_{0i} + s_{0j} - s_{ij}}{2} \tag{38}$$

where $i \neq j = 1, 2, 3, 4, 5$.

If we now calculate the eigenvalues of g_{ij}, we get $(\frac{1}{2}, \frac{1}{2}, \lambda_-, \lambda_+)$, where

$$\lambda_+ = 2\eta - \frac{1}{2} + \frac{1}{2}\sqrt{16\eta^2 - 4\eta + 1 - 12\eta\alpha + 3\alpha^2} \tag{39}$$

$$\lambda_- = 2\eta - \frac{1}{2} - \frac{1}{2}\sqrt{16\eta^2 - 4\eta + 1 - 12\eta\alpha + 3\alpha^2} \tag{40}$$

It is easy to see that since $\alpha > 1/3$ then $\lambda_+(\alpha, \eta)$ is always positive, whatever the value of η.

For λ_-, the situation is different.

- If $\eta > \eta_0$ then $\lambda_-(\alpha, \eta) > 0$
- If $\eta < \eta_0$ then $\lambda_-(\alpha, \eta) < 0$

So we see that the complex W^4 will have Euclidean signature $(+++ +)$, if $\eta > \eta_0$, and will have Lorentzian signature $(- + ++)$ if $\eta < \eta_0$.

Since there is only one internal degree of freedom, η, there is only one classical equation

$$\frac{\partial I}{\partial \eta} = 0 \tag{41}$$

which takes the form

$$\begin{aligned} T &= 8\sqrt{\frac{\alpha}{3\alpha-1}}\sqrt{\frac{\eta-\eta_0}{\eta-\alpha/4}}\Big[2\pi - 3\arccos\Big(\frac{1}{2}\frac{(4\alpha-2)\eta-\alpha^2}{(4\alpha-1)\eta-\alpha^2}\Big)\Big] \\ &+ \frac{6}{\sqrt{3\alpha-1}}\sqrt{\frac{\eta-\eta_0}{\eta-1/4}}\Big[2\pi - 4\arccos\Big(\frac{2\eta-\alpha}{2\sqrt{3\eta-1}\sqrt{(4\alpha-1)\eta-\alpha^2}}\Big)\Big] \end{aligned} \tag{42}$$

Of course the classical solutions are of the form $\eta = \eta_{cl}(\alpha, T)$ where T and α are boundary data. However, it is obvious that the previous expression does not lead to a closed expression of η as a function of α and T. So as in the previous chapters we plot the classical solutions as if T was the dependent variable and not η. Of course this changes nothing, and it serves only as a visual aid to understanding the solutions.

Note that the asymptotic behaviour of $T(\alpha_{cl}, \eta_{cl})$, when $\eta_{cl} \to +\infty$ and when $\eta_{cl} \to -\infty$, is the same

$$\begin{aligned} T(\eta_{cl} \to \infty) = T^I_{crit}(\alpha) &= \frac{8\sqrt{\alpha}}{\sqrt{3\alpha-1}}\Big[2\pi - 3\arccos\Big(\frac{2\alpha-1}{4\alpha-1}\Big)\Big] \\ &+ \frac{6}{\sqrt{3\alpha-1}}\Big[2\pi - 4\arccos\Big(\frac{1}{\sqrt{3}\sqrt{4\alpha-1}}\Big)\Big] \end{aligned} \tag{43}$$

As in the previous chapters, and for exactly the same reasons, all classical solutions occur in pairs. Each element of the pair $(\eta^I_{cl}, \eta^{II}_{cl})$, is numerically equal $\eta^I_{cl} = \eta^{II}_{cl}$, but is located respectively in the first and second sheets of the action, and so they have Euclidean actions of opposite sign $I^I[\eta^I_{cl}] = -I^{II}[\eta^{II}_{cl}]$.

For physical reasons we only consider solutions for which T is real positive and $\alpha \in [1/3, +\infty)$. By plotting the solutions we conclude that there are three different cases according to the value of α.

- CASE 1 corresponds to $\frac{1}{3} < \alpha < 1$.

  As we can see in figure 5 , in this interval there are real Lorentzian solutions for $\eta \in (-\infty, \alpha/4]$, and real Euclidean solutions for $\eta \in [\eta_0, +\infty]$. Note however that although it is not apparent in figure 5 the Euclidean solutions only obey the physical condition $T > 0$ from a value of η slightly larger than η_0. For $\eta \in [\alpha/4, \eta_0]$ and for all

non-real values of η the solutions have complex geometry. The divergence of $T(\eta_{cl}, \alpha)$ at $\alpha/4$ guarantees that there are Lorentzian solutions for all values of $T > T^I_{crit}$.

On the other hand, we have classical Euclidean solutions for all values between 0 and $T_{crit}(\alpha)$. So the existence of Euclidean solutions is limited by a ceiling $T = T^I_{crit}(\alpha)$. However, since $T^I_{crit}(\alpha \to 1/3) \to +\infty$, in this range of α we can pretty much envisage raising the ceiling as much as we want, and so there will be Euclidean classical solutions for every value of T, it is just a case of getting α ever closer to 1/3. Furthermore, note that as $\alpha \to 1/3$ the volume of the boundary tetrahedra

$$V_3[\sigma^b_3] = \frac{\sqrt{3}l^3}{12H^3}\, T^{3/2}_{crit}(\alpha)\sqrt{\alpha - 1/3}$$

does not vanish because $T_{crit}(\alpha \to 1/3) \sim (\alpha - 1/3)^{-1/4}$.

Regarding the behaviour of the action for these classical solutions it is easy to see that the Euclidean action of the Lorentzian solutions is pure imaginary.

On the other hand, the Euclidean solutions have real Euclidean action.

- CASE 2 corresponds to $1 < \alpha < 4/3$.

  The situation here is very similar to that of CASE 1, the only difference being that now the relevant critical point where the Lorentzian classical branch peaks is 1/4. As before we have Lorentzian classical solutions for values of T from T_{crit} all the way up to $+\infty$, while the existence of Euclidean classical solutions is limited to $T \in [0, T_{crit}(\alpha)]$. However, in this case the ceiling $T_{crit}(\alpha)$ is much more effective because in the range $1 < \alpha < 4/3$, $T_{crit}(\alpha)$ takes low values and there is no possibility of making it as high as we want by taking the limit $\alpha \to 1/3$, as in the previous case.

  In what concerns the action the situation is also similar to case 1. The Euclidean solutions all have real Euclidean action. As for the Lorentzian solutions they all have pure imaginary actions.

- CASE 3 corresponds to $\alpha > 1$.

  As we can see from figure 6 the situation here is different. There are two different branches of classical Lorentzian solutions $\eta_1(T, \alpha)$ and $\eta_2(T, \alpha)$ peaking respectively at the branch points $\eta = 1/4$ and $\eta = \alpha/4$. We also have the usual classical Euclidean branch, for $\eta \in [\eta_0, \infty)$.

This time the Euclidean and Lorentzian regimes are not strictly separated at the "boundary" $T = T_{crit}(\alpha)$. This is because although the Euclidean solutions are still limited to boundary data $T < T_{crit}(\alpha)$, there is now one branch of Lorentzian solutions $\eta_2(T, \alpha)$, that contains solutions for all positive values of the boundary data T, including $T < T_{crit}(\alpha)$.

Another big difference is that while the Lorentzian solutions in the $\eta_1(T, \alpha)$ branch all have real Euclidean actions, diverging to $+\infty$, as $\eta \to 1/4$, the solutions in the other Lorentzian branch $\eta_2(T, \alpha)$ have fully complex actions. The most important feature of the Euclidean action of these solutions is its behaviour near the branch point $\alpha/4$.

$$Im[I(\eta_{cl} \to \frac{\alpha}{4}^{-}, T, \alpha)] \to +\infty, \quad Re[I(\eta_{cl} \to \frac{\alpha}{4}^{-}, T, \alpha)] \to -\infty;$$

the behaviour of $ReI(\eta_{cl})$ can be seen in figure 7.

As for the Euclidean solutions, their behaviour is similar to that of the two previous cases. There are real Euclidean solutions with real Euclidean action for all the range $[\eta_0, \infty)$, but they only correspond to positive values of T for values of η slightly larger than η_0, and they are limited to a maximum value, $T_{crit}(\alpha)$, of T . In the case of $\alpha = 2$, and so $\eta_0 = 0.6$, the real Euclidean solutions only correspond to $T > 0$ from approximately $\eta = 0.631$.

Note that we have Lorentzian classical solutions for the late universe for all possible values of α. To see this remember that by late universe we mean very large boundary 3−spaces, which in our model corresponds to $a = \alpha(Tl^2/H^2) \to +\infty$. However, since we are restricted to $\alpha > 1/3$, then $a \to +\infty \Leftrightarrow T \to +\infty$.

6 Steepest Descents Contour

In this minisuperspace model the wavefunction of the Universe is

$$\Psi[T, \alpha] = \int_C D\eta \, e^{-I[\eta, T, \alpha]} \tag{44}$$

Once more this expression is only heuristic until we choose the integration contour C and the integration measure $D\eta$. As in the previous models these choices are largely independent, if we restrict our attention to polynomial measures like

$$D\eta = \frac{ds_i}{2\pi i l^2} = \frac{T}{2\pi i H^2} d\eta \tag{45}$$

In accordance with the previous chapters we shall follow Hartle's prescription for the integration contour, namely, that the correct integration contour is the steepest descents contour over complex metrics passing through the dominant extrema of the Euclidean action. We know that all classical solutions occur in pairs, $\eta_{cl}(\alpha, T) = \eta^{I}_{cl}(\alpha, T) = \eta^{II}_{cl}(\alpha, T)$, with Euclidean actions of opposite sign since they are located respectively in the first and second sheets of the action. Since by definition all points in a SD path have the same imaginary part of the action we see that no single SD path can pass through both extrema. However, if we consider a SD contour made of two complex conjugate sections one existing on the first sheet the other on the second , since, [8]:

$$I[\eta] = [I[\eta^*]]^*$$

and

$$I[\eta_I] = -I[\eta_{II}]$$

where $*$ denotes complex conjugation, we see that if one section goes through $\eta^{I}_{cl}(\alpha, T)$ the other will go through $\eta^{II}_{cl}(\alpha, T)$, and the resulting wavefunction will be real if the actions are purely imaginary or purely real.

Another way of seeing this is to remember that we are now working for $\eta \in \mathbf{R}$, and not $\eta \in \mathbb{C}$. As such, the SD contour passing through a value of $\eta_{cl}(\alpha, T)$ is

$$C_{SD}(T, \alpha) = \Big\{ \eta \in \mathbf{R} : Im[I(\eta, T, \alpha)] = Im[I(\eta_{cl}(T, \alpha), T, \alpha)] \Big\} \tag{46}$$

it is then easy to conclude from our knowledge of the behaviour of the action in the several sheets of $\mathbf{R}$ that if C_{SD} passes through η^{I}_{cl} in $\mathbb{C}_1$ it will pass through η^{II}_{cl}in $\mathbb{C}_2$.

For brevity we shall display only the SD contours associated with the classical solutions in the range $\alpha > 4/3$, ie., case 3, because the contours associated with the cases 1 and 2 are similar to the contours associated with case 3.

In figure 8 we present the SD contour passing through the classical Lorentzian solution $\eta^{1}_{cl}(T = 100, \alpha = 2) = 0.2401$, belonging to the first branch of Lorentzian solutions that peaks at $\eta = 1/4$.

Starting off at the real Lorentzian classical solution $\eta_{cl}(T = 100, \alpha = 1) = 0.2401$, if we move upwards the SD contour goes to infinity in the first quadrant along the parabola

$$\frac{\sqrt{3\alpha-1}}{H^2}T[T-T^I_{crit}(\alpha)]\sqrt{\eta}=\tilde{I}[\eta_{cl}=0.2401]=265.71 \tag{47}$$

where $\tilde{I}=Im(I)$.

The convergence of the integral along this part of the SD contour is guaranteed by the asymptotic behaviour of the action

$$Re[I^I(\eta\to\infty,\alpha,T)]\sim\frac{\sqrt{3\alpha-1}}{H^2}T[T-T^I_{crit}(\alpha)]\sqrt{\mid\eta\mid} \tag{48}$$

since for this branch of Lorentzian solutions we always have $T>T^I_{crit}(\alpha)$, and in particular $T^I_{crit}(\alpha=2)=17.03$.

If instead we move downwards from the classical solution we immediately cross onto the second sheet of the action, where the SD contour encircles the branch point $\eta=1/4$ crossing the branch cut $(-\infty,\eta_0]$ once more, this time between $1/4$ and $\alpha/4=1/2$, at $\eta=0.2632$. When it does so it emerges onto the third sheet of the action where it goes to infinity in the first quadrant along the parabola

$$\frac{\sqrt{3\alpha-1}}{H^2}T[T-T^{III}_{crit}(\alpha)]\sqrt{\eta}=\tilde{I}[\eta_{cl}=0.2401]=265.71 \tag{49}$$

Once more the convergence of the integral along this part of the SD contour is guaranteed by the asymptotic behaviour of the action in the third sheet

$$Re[I^{III}(\eta\to\infty,\alpha,T)]\sim\frac{\sqrt{3\alpha-1}}{H^2}T[T-T^{III}_{crit}(\alpha)]\sqrt{\mid\eta\mid} \tag{50}$$

since T^{III}_{crit} is always small or negative. In this particular case $T^I_{crit}(\alpha=2)=-16.69$

The other section of this SD contour passing through the other extremum located at the second sheet is just the complex conjugate of this contour and so we will not show it here.

We now study the SD contours associated to the second branch of classical Lorentzian solutions, i.e., the one that peaks at $\eta=\alpha/4$.

In figure 9 we display the SD contour associated with the Lorentzian classical solution $\eta^2_{cl}(T=100,\alpha=0.4931)$. Moving upwards we again go to infinity in the first quadrant of the first sheet along the parabola

$$\frac{\sqrt{3\alpha-1}}{H^2}T[T-T^I_{crit}(\alpha)]\sqrt{\eta}=\tilde{I}[\eta_{cl}=0.4931]=165.53 \tag{51}$$

The convergence of the integral is guaranteed by the asymptotic behaviour of the action in the first sheet

$$Re[I^I(\eta \to \infty, \alpha, T)] \sim \frac{\sqrt{3\alpha - 1}}{H^2} T[T - T^I_{crit}(\alpha)]\sqrt{\mid \eta \mid} \tag{52}$$

given that $T_{crit}(\alpha = 2) = 17.03$.

However, if we move downwards we cross the branch cut and emerge onto what we have defined as the fourth sheet of the action. There the SD contour encircles the branch point $\alpha/4 = 0.5$, and moves upward to cross the branch cut again between the branch points $\alpha/4 = 0.5$ and $\eta_1(\alpha = 2) = 0.571$, more specifically at $\eta = 0.5175$. By doing this it moves onto the fifth sheet, where once more it goes to infinity in the first quadrant along the parabola

$$\frac{\sqrt{3\alpha - 1}}{H^2} T[T - T^V_{crit}(\alpha)]\sqrt{\eta} = \tilde{I}[\eta_{cl} = 0.4931] = 165.53 \tag{53}$$

The convergence of the SD contour along this section is assured by the asymptotic behaviour of the action in this fifth sheet

$$Re[I^V(\eta \to \infty, \alpha, T)] \sim \frac{\sqrt{3\alpha - 1}}{H^2} T[T - T^V_{crit}(\alpha)]\sqrt{\mid \eta \mid} \tag{54}$$

This is because $T^V_{crit}(\alpha)$ is always negative. In this particular case $T^V_{crit}(2) = -46.55$.

In the case of the Euclidean classical solutions they also occur in pairs but since they both have real Euclidean action they can both lie in the same SD path because the imaginary part of the action is equal for both of them, i.e., zero.

In figure 10, we present the SD contour associated with the pair of Euclidean classical solutions, numerically equal to

$$\eta^{sheetI}_{cl}(T = 13, \alpha = 2) = \eta^{sheetII}_{cl}(T = 13, \alpha = 2) = 1.180$$

but located in the first and second sheets, and so with real Euclidean actions of opposite sign, $I[\eta^{sheetI}_{cl}(T = 13, \alpha = 2)] = -I[\eta^{sheetII}_{cl}(T = 13, \alpha = 2)] = -4.033$.

We see that starting at the classical solution $\eta^{sheetI}_{cl}(T = 13, \alpha = 2) = 1.180$, if we move upwards in the first sheet the SD contour encircles all branch points and crosses the branch cut $(-\infty, \eta_0 = 0.6]$ at $\eta = -0.2638$, emerging onto the second sheet where it encircles all branch points in the opposite direction and arrives at the second classical solution $\eta^{sheetII}_{cl}(T = 13, \alpha = 2) = 1.180$. If we do another loop we will cross back onto the first sheet and will arrive back where we started, i.e., at the classical solution in the first sheet $\eta^{sheetI}_{cl}(T = 13, \alpha = 2) = 1.180$. So the SD contour is clearly closed. Since there are

no other critical points of the action in this SD contour we do not need to worry about the contribution (to the path integral) of any more points other than the two classical solutions.

7 Semiclassical Wavefunctions

We have proved that for any classical solution there is always an SD contour passing through it. Furthermore by analysis of the asymptotic behaviour of the action we have been able to establish that any path integral along such SD contours will always be convergent, since none of them crosses any singularities and the contribution from the infinities is vanishing.

However this is not enough to prove that the semiclassical approximation is always a good approximation of the SD wavefunction. In order to do that we must prove that the contributions from the regions about the classical solutions are clearly dominant, when compared with the contribution from the rest of the SD contour. For this to happen the values of T, α and H must be such that, locally, the integrand, i.e., $\exp -I$ is sharply peaked about the extrema.

In our case the classical solutions always occur in pairs with actions of opposite sign. If these solutions are Lorentzian and have pure imaginary Euclidean actions, $I[\eta_{cl}, T, \alpha] = ImI[[\eta_{cl}, T, \alpha]$, then for the linear CPT symmetric wavefunction of the no boundary proposal we expect the real combination of these two contributions. So the semiclassical wavefunction takes the form

$$\Psi_{SC}(T,\alpha) \sim \sqrt{\frac{T^2}{2\pi H^4 \mid I''[\eta_{cl}(T,\alpha)] \mid}} 2\cos\left\{ ImI[\eta_{cl}(T,\alpha),\ T,\alpha]\right\} \tag{55}$$

where $'$ denotes $d/d\eta$.

This is what happens for semiclassical approximations based on the the Lorentzian classical solutions in cases 1 and 2, i.e., when $\alpha \in (1/3, 1]$, and $\alpha \in [1, 4/3]$. It is also what happens in case 3, $(\alpha > 4/3)$, for the first branch of Lorentzian solutions peaking at $\eta = 1/4$. In figures 11 and 12 we can see some examples of these wave functions.

The semiclassical approximation is good when $\exp(-I)$ is sharply peaked about the extrema, i.e., when $ImI[\eta_{cl}(T,\alpha)]$ is large. This will always be the case for the late universe . If for example we consider $\alpha = 1$ then for the late universe where $T \to +\infty$ and $\eta_{cl}^{Lor} \to 1/4$, the action takes the form

$$ImI_{cl}(T,\alpha=1) \sim \frac{T^2}{2H^2} = \frac{1}{2}(\Lambda\, b^2/l^2) \tag{56}$$

So the semiclassical approximation will be very good for large values of T. It will also be the case over the whole range of T, (except for T_{crit}), when $H^2 = \Lambda l^2/3$ is sufficiently small as it certainly is in our late universe.

However we can see in figures 11 and 12 that the semiclassical wavefunctions diverge as $T \to T^I_{crit}$, but that is only a symptom that the semiclassical approximation breaks down there, which is signalled by the fact that $I''[\eta_{cl}(T,\alpha) \to 0$ when $T \to T^I_{crit}$.

An oscillating wavefunction of the kind in figures 11 and 12 predicts classical Lorentzian spacetime for the late universe, described by the Lorentzian classical solutions computed above. What does it say about the evolution of the wormhole? Well since our late universe corresponds to large 3−boundaries, which is the case for our classical solutions when $T = bH^2/l^2 \to +\infty$ and $a = \alpha b \to +\infty$, then it seems that the wormhole throat will grow with the expansion of the Lorentzian twin universes. So this wavefunction does not predict the collapse of the wormhole.

When the classical solutions come in pairs of Euclidean solutions with real valued actions of opposite sign, as in the regions $\eta \in [\eta_0, +\infty)$ where $0 < T < T^I_{crit}$, the solution with negative real Euclidean action will always dominate over its counterpart. In our case the action of the Euclidean solutions in the first sheet is always negative, and so the solutions on the first sheet will dominate over the ones in the second sheet.

However, as discussed above, the semiclassical approximation based on these solutions, will only be valid if the region near them gives the dominant contribution to the full SD contour integration. This only happens when the action is strongly peaked in the SD section around them. Since we are now limited to $T < T^I_{crit}$, this is only true when H^2 is small.

And so the asymptotic behaviour of (44) for small H^2 is given by the semiclassical approximation associated with the Euclidean solution in the first sheet, $\eta^{sheetI}_{cl}(T,\alpha)$

$$\Psi^{Eucl}_{SC}(T,\alpha) \sim \sqrt{\frac{T^2}{2\pi H^4 \mid I''[\eta_{cl}(T,\alpha)] \mid}}\, e^{-I[\eta^{sheetI}_{cl}(T,\alpha),\, T,\alpha]} \tag{57}$$

The second derivative of the action vanishes as $T \to T^I_{crit}$, and so it will be this term that will dominate the semiclassical wavefunction near the "turning point", T^I_{crit}, and lead to its divergence there. However, when H is small, the $exp(-I)$ term is dominant everywhere except when T is really close to T^I_{crit}. For small H the real valued Euclidean action peaks

around the Euclidean classical solution and so the semiclassical approximation is good for almost all values of T, except when we get too close to T^I_{crit}.

In figure 13 we see the plot of this semiclassical wavefunction for $\alpha = 2$ and $H = 4.9$. There is a clear peak away from T^I_{crit}, at $T = 13.35$, where the semiclassical approximation is valid, which seems to indicate a preferred value of the boundary edges $b = Tl^2/H^2$ and consequently $a = b\alpha = 2b$. This peak becomes more pronounced as H becomes smaller. We thus seem to have a prediction of a favoured size of the wormhole throat, when we are dealing with wormholes between Euclidean universes.

We now discuss a third kind of classical solutions. When $\alpha > 4/3$, we know that there are two branches of Lorentzian classical solutions, branch 1 peaking at $\eta = 1/4$ and branch 2 peaking at $\eta = \alpha/4$. These solutions in the second branch have fully complex Euclidean actions.

$$I[\eta_2^{cl}(T,\alpha)] = ReI[\eta_2^{cl}(T,\alpha)] + iImI[\eta_2^{cl}(T,\alpha)]$$

Their counterparts on the second sheet will also have complex actions, but of opposite sign. So no linear combination of the contribution from these two solutions will ever lead to a real wavefunction. Moreover since the real part of the Euclidean action is always negative for the classical solutions $\eta_2^{cl}(T,\alpha)$ on the first sheet, even diverging to $-\infty$, as $\eta \to \alpha/4$, as can be seen in figure 7, it seems obvious that the extremum in the first sheet will dominate the path integral.

In order to understand a little better this situation we need to do a slight diversion, [16].

The starting point of a semiclassical/WKB approximation is to assume that the full wavefunction is well approximated by the contribution of the regions about some finite number of classical extrema. In our case it is just one and so the wavefunction can always be written as

$$\Psi[h_{ij}] = C \exp \frac{-I[h_{ij}]}{\hbar} \tag{58}$$

where $I = I_r + iI_i$, where I_r and I_i are the real and imaginary parts of the Euclidean action, and the pre-factor C is a slowly varying amplitude containing all higher-order corrections.

At the level of the first approximation in $\hbar$ the Wheeler-DeWitt equation on $\Psi[h_{ij}]$ is then reduced to the classical Hamilton-Jacobi equation on I, [17].

$$H_0\left(\pi^{ij} = i\frac{\delta I}{\delta h_{ij}}, h_{ij}\right) = 0 \tag{59}$$

$$\left[G_{ijkl}\frac{\delta I}{\delta h_{ij}}\frac{\delta I}{\delta h_{kl}} + \sqrt{h}({}^3R - 2\Lambda)\right] = 0 \tag{60}$$

where $G_{ijkl} = \frac{1}{2\sqrt{h}}(h_{ik}h_{jl}+h_{il}h_{jk}-h_{ij}h_{kl})$ and the π^{ij} are the canonical conjugate momenta of h_{ij}.

The action $I[h_{ij}]$ that solves the the Hamilton-Jacobi equation is the classical action of a congruence of solutions, $[h_{ij}(t)]$, of the classical equations of motion. These trajectories, parametrised by their coordinate time t, are defined by

$$\pi^{ij} = i\frac{\delta I}{\delta h_{ij}} \tag{61}$$

If the action I is real, the wavefunction has an exponential form and can be formally interpreted as an ensemble of classical Euclidean solutions/trajectories. If the action I is pure imaginary, then the wavefunction has oscillatory behaviour, and describes an ensemble of classical Lorentzian solutions.

However, if the action I is fully complex the Hamilton-Jacobi equation can be decomposed into the real part

$$(\nabla I_r)^2 - (\nabla I_i)^2 + \sqrt{h}({}^3R - 2\Lambda) = 0 \tag{62}$$

and the imaginary part

$$(\nabla I_r) \times (\nabla I_i) = 0 \tag{63}$$

From 62, we can see that if the gradient of I_i becomes much larger than the gradient of I_r, then I_i will be an approximate solution to the Hamilton-Jacobi equation. This means that the classical evolution is almost Lorentzian.

If I defines an ensemble of almost Lorentzian solutions, then the real part of the action is also relevant, since it will contribute the term $\exp(-I_r)$ to the pre-factor. Since it is exponential it will probably be the dominant contribution to the pre-factor. Then the probability measure provided by the pre-factor on the ensemble of classical solutions is, to leading order, of the form $\exp(-2I_r)$, determining the relative weight of different trajectories.

This is exactly what happens in the case of branch 2 of classical solutions, $\eta_2^{cl}(T,\alpha)$ when $\alpha > 4/3$. As can be seen in figure 14, the ratio R between the gradients of the imaginary and real parts of the Euclidean action

$$R = \frac{\mid \nabla ImI[\eta = \eta_2^{cl}] \mid}{\mid \nabla ReI[\eta = \eta_2^{cl}] \mid} \tag{64}$$

along the classical solutions of branch 2, becomes infinitely large for the late universe, i.e., for $a = \alpha(Tl^2/H^2) \to +\infty \Leftrightarrow \eta_2^{cl} \to \frac{\alpha}{4}^-$. So for the late universe ImI really solves the classical Hamilton-Jacobi equation. And so the wavefunction should describe an ensemble of Lorentzian solutions for the late universe.

The contribution of the imaginary part of the action to the wavefunction does indeed yield the characteristic oscillating behaviour associated with the prediction of classical Lorentzian spacetime for the late universe, as can be seen in figure 15.

The real part of the action provides the probability measure, $\exp\{-2ReI[\eta_2^{cl}]\}$, on the ensemble of classical Lorentzian universes, determining the relative weight of these different trajectories. From figure 7, we see that $\exp\{-2ReI[\eta_2^{cl}]\}$ becomes infinitely large as $T \to +\infty$, since $ReI[\eta_2^{cl}] \to -\infty$ as $\eta_2^{cl} \to \frac{\alpha}{4}^-$. It thus seems that in this model, when $\alpha > 4/3$ if we choose the classical solutions of branch 2 as the basis for the semiclassical approximation of the wavefunction of the universe, then configurations consisting of extremely large Lorentzian classical universes connected by similarly large wormholes will dominate.

8 Conclusions

The minisuperspace approximation comes very naturally in simplicial quantum gravity, because by discretising spacetime we are in effect substituting the functional $h_{ij}(\mathbf{x},t)$, by a set of simple variables, the edge lengths. The minisuperspace approximation consists only in restricting all these edge lengths to being equal to a small number of parameters. So the loss of generality is much smaller than when we impose the minisuperspace approximation to the continuum. Furthermore, in the simplicial minisuperspace, spacetime continues to be treated in a fully $4-$dimensional way. There is no need to invoke any arbitrary $3+1$ decomposition of spacetime, usually ADM, as in the case of continuum models. This means that global issues like topology can still be addressed in the simplicial minisuperspace, which is not possible in the continuum versions. The versatility of our approach is evident in the ease in which one can construct a $4-$D wormhole configuration. Furthermore, since the

signature of the simplicial spacetime is only dependent on the ratio between edge lengths, we can deal with Lorentzian and Euclidean configurations at the same time. Indeed with the same model we were able to study microscopic Euclidean wormholes and large Lorentzian wormholes.

The simplicial geometry used is quite simple and so it cannot take into account some relevant dynamics that we would like to model. In particular it would be better if we could have developed a solvable model with an additional interior edge length, that would describe the throat of the wormhole. However, we decided that before we considered that much more complicated model it would be very useful to determine the results of the simplest model. And indeed we found several new and interesting results. For Euclidean wormholes just above the Planck scale, there is a strongly preferred non-zero throat size. As H becomes smaller the peak becomes sharper, and we obtain a very stable configuration. Thus the model predicts that Euclidean wormholes of that scale are stable insofar as that their throat do not tend to contract leading to the pinching off of the two universes.

For large Lorentzian wormhole configurations the situation is dependent on the value of $\alpha = a/b$. If $\alpha \in [1/3, 4/3]$, then there is only one family of Lorentzian solutions, all with pure imaginary Euclidean action. The semiclassical wavefunction is a very good approximation of the full wavefunction for the late, large Lorentzian universes. Its oscillating behaviour definitely predicts classical Lorentzian configurations for large universes, with a similarly large wormhole throat connecting them. However, when $\alpha > 4/3$, a new family of Lorentzian solutions is present. The fact that their Euclidean action is fully complex, with a real part that diverges when the boundary $3-$space becomes large, (i.e. late universe), seems to indicate that these solutions will dominate the path integral leading to the full wavefunction. A semiclassical interpretation of the resulting wavefunction is that it describes an ensemble of classical Lorentzian spacetimes, weighted by $\exp(-2ReI)$. Since this exponential diverges to $+\infty$ for increasingly large $3-$spaces, we can conclude that large wormhole configurations between very large Lorentzian universes are very strongly favoured.

References

[1] S. Coleman, Nucl.Phys.B**310** (1988) 643.

[2] J.P. Preskill, Nucl.Phys.B**323** (1989) 141.

[3] S.W. Hawking, Nucl.Phys.B**335** (1990) 155.

[4] W. Fischler and L. Susskind, Phys.Lett.B**217** (1989)48.

[5] R. Grinstein, Nucl.Phys.B**321** (1989) 429.

[6] D. Hochberg, Phys.Rev.D**52** (1995) 6846.

[7] D. Hochberg and M. Visser, Phys.Rev.D**56** (1997) 936.

[8] J.B.Hartle, J.Math.Phys **30** (1989) 452.

[9] D.Birmingham, Phys.Rev.D**52** (1995) 5760.

[10] C.C.da Silva, R.M. Williams, Class.Quantum Grav**16**(1999) 2681.

[11] J.B.Hartle, Class. Quantum Gravity **2** (1985) 707.

[12] K. Schleich and D.M. Witt, Nucl. Phys. B**402**(1993) 469.

[13] C.C.da Silva, R.M. Williams, Class.Quantum Grav**16**(1999) 2197.

[14] C.C.da Silva, R.M. Williams, CQG/110370/PAP(2000)gr-qc 0002084

[15] J.J. Halliwell and J.B. Hartle, Phys.Rev.D**41** (1990) 1815.

[16] J.J.Halliwell in *Proceedings of the Jerusalem Winter School on Quantum Cosmology and Baby Universes*, ed. by T. Piran (World Scientific, Singapore 1990).

[17] T. Banks , Nucl.Phys.B**249** (1984) 339.

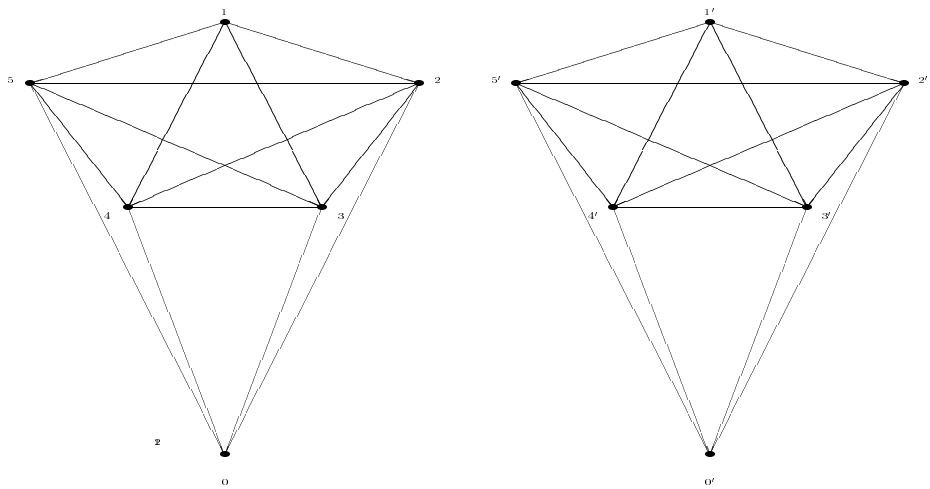

Figure 1: Figure 1: Two copies $\mathcal{C}_1$ and $\mathcal{C}_2$ of an isotropic simplicial universe that triangulates an open $4-$ball.

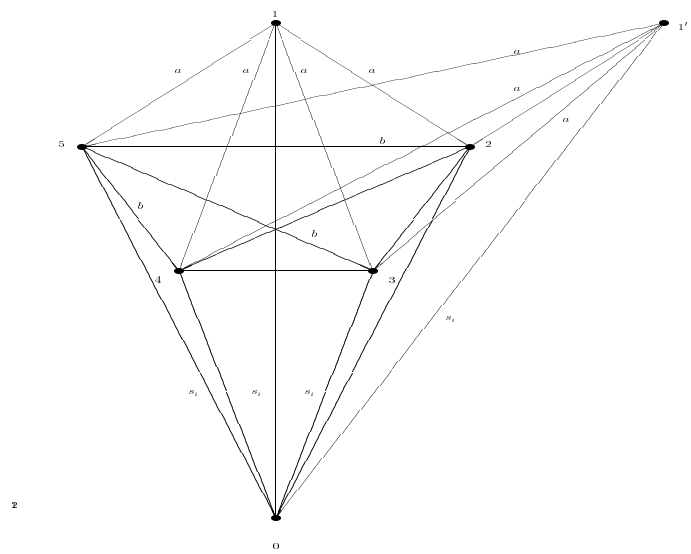

Figure 2: Figure 2: Simplicial wormhole configuration W^4.

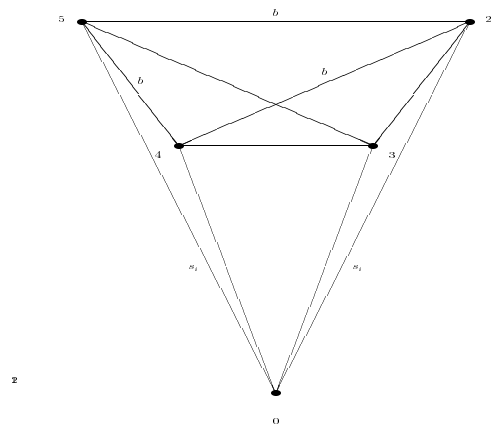

Figure 3: Figure 3: The throat T^3 connecting $\mathcal{C}_1$ and $\mathcal{C}_2$.

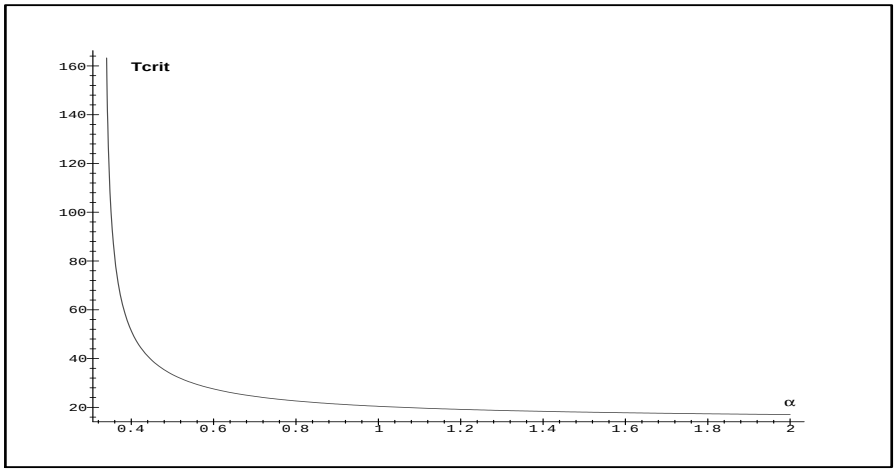

Figure 4: T^I_{crit} as a function of α. Note that its asymptotic value is 14.51.

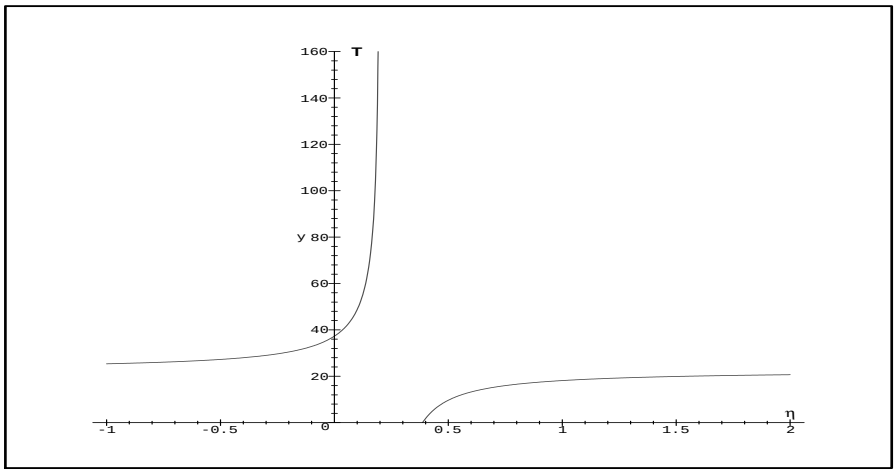

Figure 5: Classical solutions for $\alpha = 0.8$

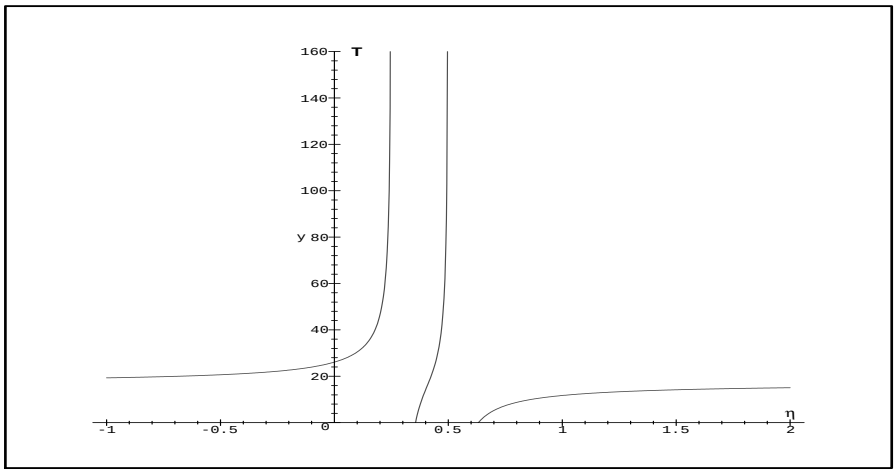

Figure 6: Classical solutions for $\alpha = 2$

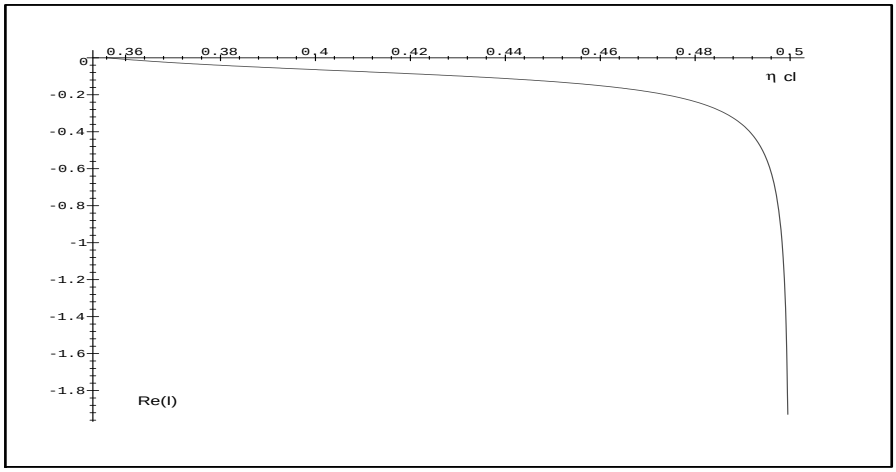

Figure 7: Real part of the complex Euclidean action for the Lorentzian classical solutions of branch 2, between 1/4 and $\alpha/4$, for $\alpha = 2$

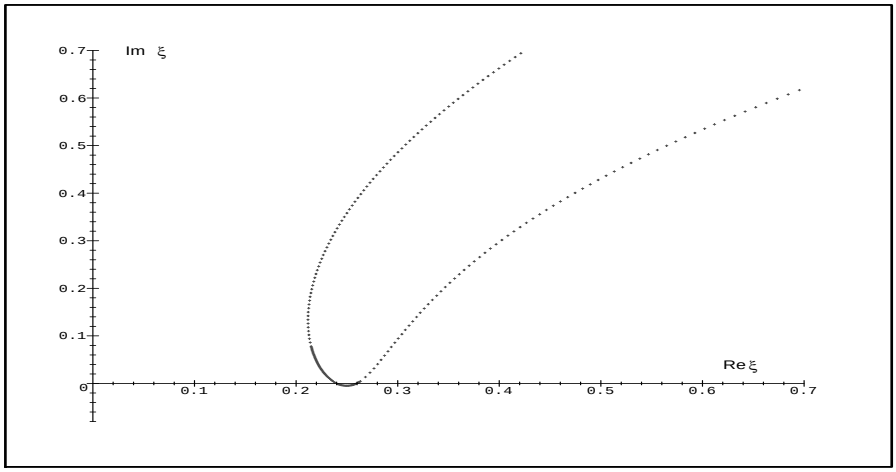

Figure 8: Steepest Descents contour for the classical solution $\eta^1_{cl}(T = 100, \alpha = 2) = 0.2401$

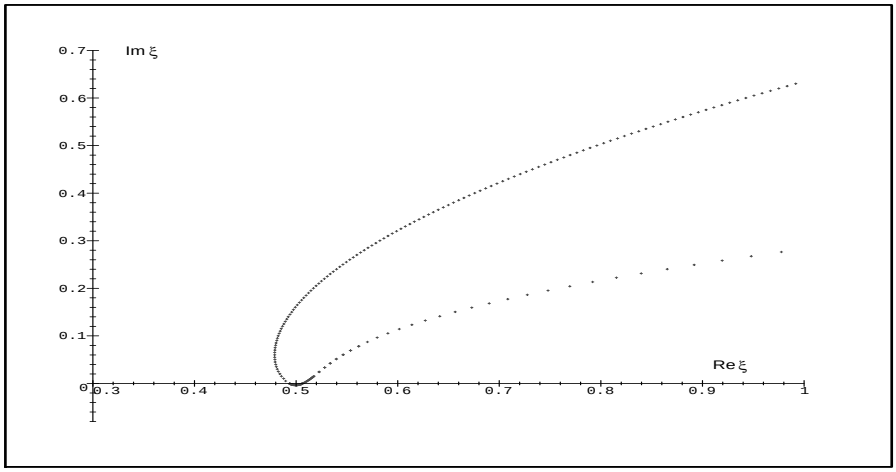

Figure 9: Steepest Descents contour for the classical solution $\eta_{cl}^2(T = 100, \alpha = 2) = 0.4931$

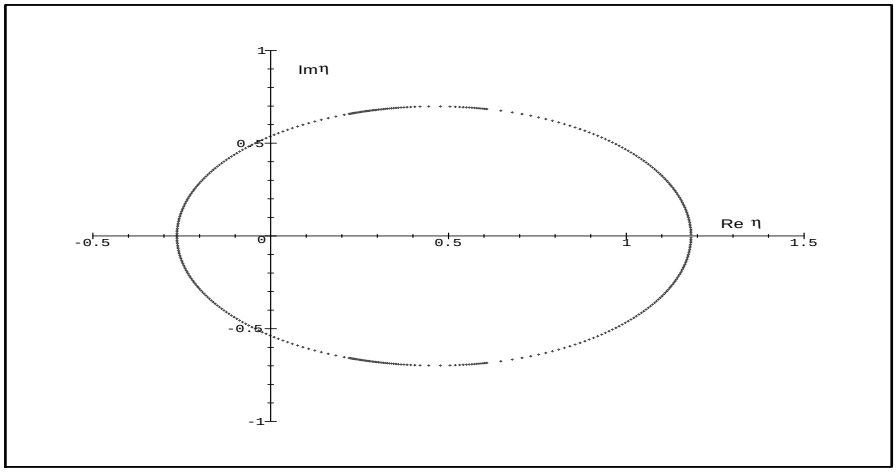

Figure 10: Steepest descents contour for the Euclidean classical solution$\eta_{cl}(T = 13, \alpha = 2) = 1.180$

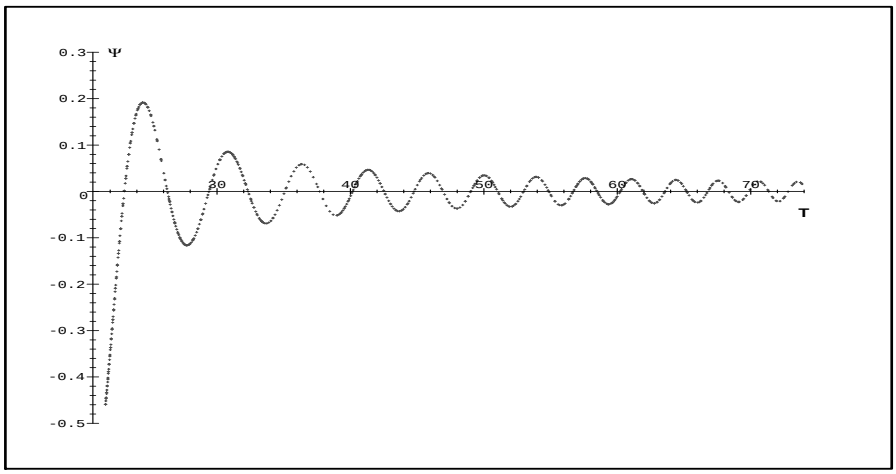

Figure 11: Semiclassical wavefunction based on the Lorentzian solutions for $\alpha = 1.2$ and $H = 7$

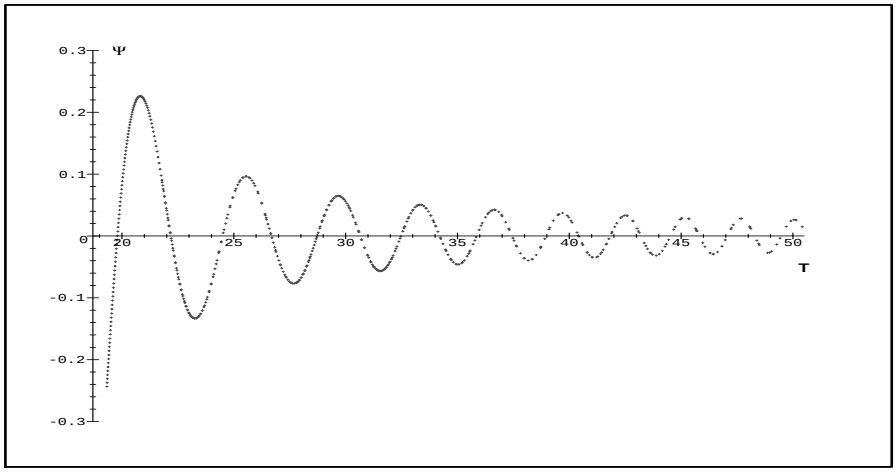

Figure 12: Semiclassical wavefunction based on the branch 1 Lorentzian solutions, ($\eta < 1/4$), for $\alpha = 2$ and $H = 7$.

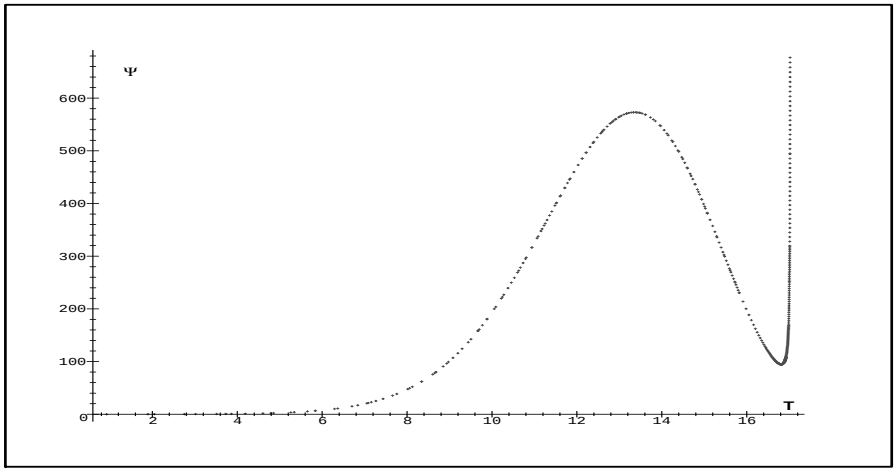

Figure 13: Semiclassical wavefunction based on the Euclidean solutions for $\alpha = 2$ and $H = 4.9$

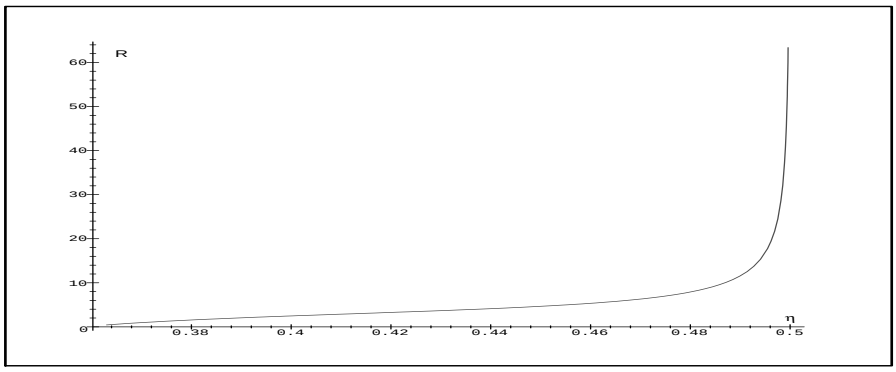

Figure 14: Ratio R of the gradient of Im(I) over the gradient of Re(I), along the classical solutions of branch 2, η_2^{cl}, for $\alpha = 2$. Note how much larger the gradient of Im(I) becomes, as we approach the late Universe, i.e., when $T \to +\infty \Leftrightarrow \eta \to \alpha^-/4$.

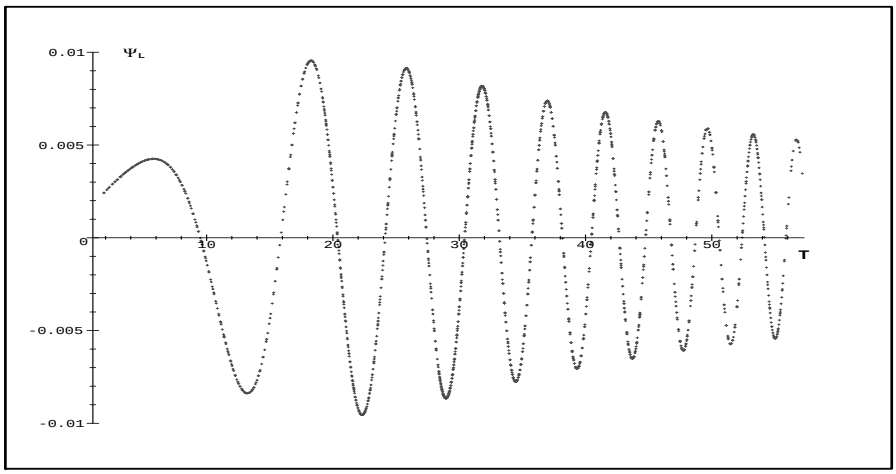

Figure 15: Lorentzian part of the semiclassical wavefunction, describing an ensemble of classical Lorentzian universes